

# Journal of Biomedical Optics

[SPIEDigitalLibrary.org/jbo](http://SPIEDigitalLibrary.org/jbo)

## **Consistency and distribution of reflectance confocal microscopy features for diagnosis of cutaneous T cell lymphoma**

Susanne Lange-Asschenfeldt  
Jasmin Babilli  
Marc Beyer  
Francisca Ríus-Díaz  
Salvador González  
Eggert Stockfleth  
Martina Ulrich

# Consistency and distribution of reflectance confocal microscopy features for diagnosis of cutaneous T cell lymphoma

Susanne Lange-Asschenfeldt,<sup>a</sup> Jasmin Babilli,<sup>a</sup> Marc Beyer,<sup>a</sup> Francisca Ríus-Díaz,<sup>b</sup> Salvador González,<sup>c</sup> Eggert Stockfleth,<sup>a</sup> and Martina Ulrich<sup>a</sup>

<sup>a</sup>Universitätsmedizin Charité, Department of Dermatology, Berlin, Germany

<sup>b</sup>University of Malaga, Department of Biostatistics, Malaga, Spain

<sup>c</sup>Memorial Sloan Kettering Cancer Center, Division of Dermatology, New York, New York

**Abstract.** Reflectance confocal microscopy (RCM) represents a noninvasive imaging technique that has previously been used for characterization of mycosis fungoides (MF) in a pilot study. We aimed to test the applicability of RCM for diagnosis and differential diagnosis of MF in a clinical study. A total of 39 test sites of 15 patients with a biopsy-proven diagnosis of either MF, parapsoriasis, Sézary syndrome, or lymphomatoid papulosis were analyzed for presence and absence of RCM features of MF. Cochran and Chi<sup>2</sup> analysis were applied to test the concordance between investigators and the distribution of RCM features, respectively. For selected parameters, the Cochran analysis showed good concordance between investigators. Inter-observer reproducibility was highest for junctional atypical lymphocytes, architectural disarray, and spongiosis. Similarly, Chi<sup>2</sup> analysis demonstrated that selected features were present at particularly high frequency in individual skin diseases, with values ranging from 73% to 100% of all examined cases. © 2012 Society of Photo-Optical Instrumentation Engineers (SPIE). [DOI: 10.1117/1.JBO.17.1.016001]

Keywords: reflectance confocal microscopy; mycosis fungoides; parapsoriasis; cutaneous lymphoma.

Paper 11522 received Sep. 19, 2011; revised manuscript received Oct. 28, 2011; accepted for publication Nov. 2, 2011; published online Jan. 31, 2012.

## 1 Introduction

Mycosis fungoides (MF) represents the most common of cutaneous T-cell lymphomas, constituting 44%<sup>1</sup> of all diagnoses. Routinely, a classification is obtained on histological, molecular genetics, and immune-phenotypic grounds,<sup>2</sup> yet differential diagnosis is broad, including a number of eczematous skin conditions, psoriasis, or parapsoriasis. In addition, there is an inherent heterogeneity of MF lesions, often expressing subtle histological features that mimic those of other inflammatory or neoplastic skin conditions.

Previous studies have reassessed the diagnostic impact of histological parameters of MF, whereby it was shown that only selected features ultimately play a role in the differential diagnosis of MF. While one study has attributed a distinctive role to the presence of haloed lymphocytes as the most characteristic feature,<sup>3</sup> others have suggested a combination of criteria such as epidermotropism, band-like or patchy inflammatory infiltrate along the dermo-epidermal junction (DEJ), and the presence of papillary dermal fibrosis as most likely to detect early lesions of MF on routine histology.<sup>4</sup> Pautrier's microabscesses are regarded as a specific finding of MF; however, they are only present in a minority of cases,<sup>3-5</sup> and mostly in more advanced lesions of plaque-stage MF.

A discrete clinical aspect of early patch-stage MF, together with inconclusive histological findings often prompt multiple

sequential biopsies to establish diagnosis, often delaying the initiation of appropriate therapeutic management for years or decades. Beside the difficulties of obtaining MF diagnosis in early stages, heterogeneity of MF lesions seems to play a major role. In a study by Massone et al. two or more biopsies of different MF lesions were performed at different body sites at the same day, revealing different histopathologic aspects.<sup>4</sup> Therefore, the selection of the biopsy site is crucial to avoid sampling errors and establish accurate diagnosis.<sup>6</sup> In that regard, it was suggested that noninvasive imaging prior to excision may aid in the selection of biopsy sites and decrease the number of false-negative test results. Reflectance confocal microscopy has previously been used for noninvasive characterization of MF in a pilot study by Agero et al. (2007), whereby RCM features of MF were described in correlation with routine histology.<sup>7</sup> Good correlations were found between the presence of atypical lymphocytes in epidermal, junctional or dermal distribution, Pautrier's microabscesses, and dermal features such as blood vessel dilation and fibrosis. However, data on their clinical applicability and diagnostic reliability is currently lacking.

This study was designed to study the diagnostic applicability of RCM for cutaneous T-cell lymphoma. By basing our observations on those RCM parameters first published by Agero et al. for the characterization of MF, we set out to test their reproducibility, consistency, and distribution in a clinical study using blinded image analysis followed by a sensitivity/specificity analysis for all relevant parameters.

Address all correspondence to: Martina Ulrich, Charité—Universitätsmedizin Berlin, Department of Dermatology, Charitéplatz 1, DE-10117, Berlin, Germany. Tel: +49 519 888 4567 x 37517; Fax: +49 519 746 8115; E-mail: martina.ulrich@charite.de

## 2 Materials and Methods

### 2.1 Participants

Fifteen ( $n = 15$ ) patients with a biopsy-proven diagnosis of either MF ( $n = 10$ ), parapsoriasis en petite plaque ( $n = 3$ ), Sézary syndrome ( $n = 1$ ), or lymphomatoid papulosis (LYP Type A,  $n = 3$ ) were enrolled in this study. Two patients had both MF and lymphomatoid papulosis. One or more test sites were evaluated in each patient and, following clinical and RCM evaluation and the analysis of nine normal skin sites, acted as controls. Therefore, a total of 39 test sites were included in the final analysis. The research protocol was approved by the Charité University Hospital Subcommittee on Human Studies, at the Institutional Review Board. Subjects with a history of significant other erythrosquamous skin disease, including psoriasis or eczema, were excluded from the protocol. Consent was obtained prior to enrollment and all clinical investigation was conducted according to the Declaration of Helsinki Principles.

### 2.2 Evaluation Protocol

#### 2.2.1 *In vivo* RCM evaluation

A commercially available *in-vivo* RCM device (Vivascope® 1500, Lucid-Tech Inc., Henrietta, NY; Mavig GmbH Munich, Germany) was used for imaging. A detailed description of this technique and the device used has previously been published.<sup>8–10</sup> RCM evaluation was performed at lesional skin as well as clinically noninvolved corresponding skin sites. If site-matched contralateral control skin sites were unavailable, the closest unaffected skin in the surrounding area was selected for imaging.

Each skin site was systematically evaluated by RCM: a systematic horizontal mapping ( $4 \times 4$  mm to  $8 \times 8$  mm) was performed at the granular and spinous layers, at the DEJ, and at the level of the superficial dermis using the Vivablock® function. Furthermore, vertical mapping using Vivastack® function was performed in  $5\text{-}\mu\text{m}$  steps to a maximum depth of  $200\ \mu\text{m}$  beginning with the stratum corneum, through the entire epidermis, and into the upper reticular dermis. At areas of special interest individual images were captured during the imaging process. The sites were evaluated with regard to the presence or absence of diagnostic RCM criteria for MF,<sup>7</sup> and a score of 0 or 1 was assigned to each parameter.

**Blinded scoring.**—Two assessors (INV I + II) were blinded to participant name, age, sex, and suspected diagnosis and were randomly given images for assessment. Before scoring, the assessors were instructed in the interpretation of RCM images by the primary investigator using a training set with representative images of each individual RCM parameter. For each patient, three to four images of each layer, as well as complete Vivablocks® and Vivastacks®, were selected by the primary investigator for blinded assessment. Thereby a score of either absent (–) or present (+) was assigned to each individual parameter using a scoring sheet and including all parameters listed in Table 1.

### 3 Statistical Analysis

Concordance between different evaluators was determined using the Cochran test. Data from the primary investigator, as well as

two blinded observers, were included in the analysis. With respect to this study, the null hypothesis ( $H_0$ ) assumes that two observers would come to a similar diagnosis, such that  $p$ -values  $>0.05$  indicate that  $H_0$  cannot be rejected, thereby indicating homogeneity between investigators with respect to the selected parameter. On the other hand,  $p$ -values  $<0.05$  indicate that  $H_0$  can be rejected, whereby no relevant inter-observer concordance may be demonstrated for the selected parameter.  $\text{CHI}^2$  test was performed to analyze the distribution of RCM features in selected skin diseases (MF, parapsoriasis, lymphomatoid papulosis, Sézary Syndrom) and normal skin, respectively. Analysis was made for each individual RCM parameter and each investigator. For this analysis,  $H_0$  assumes that all parameters are distributed evenly between different skin diseases. Level of significance was set at  $p < 0.05$ , whereby the  $H_0$  can be rejected, indicating that the selected feature is not evenly distributed. Data were expressed for all RCM parameters.

Sensitivity and specificity analysis was performed using crosstabs; only data from blinded evaluations (INV I + II) were included in the analysis. Data were expressed as % with respective  $p$ -values from Pearson Chi-Square test; level of significance was set at  $p < 0.05$ .

All data analysis was performed using a SPSS statistical software package for Windows (SPSS Inc., Chicago, Illinois).

## 4 Results

Following clinical and RCM evaluation, 15 patients with a total number of 39 test sites were included in the final analysis. Correct diagnosis of MF by blinded images analysis through the two independent observers was obtained in 84% and 90% of cases, respectively. A total number of five lesions were misdiagnosed, whereby four cases were misclassified as parapsoriasis and one case as normal skin.

## 5 Concordance Analysis

The Cochran Test included RCM scorings from the primary investigator and two blinded investigators. For selected parameters, the Cochran homogeneity analysis showed concordance between investigators (Table 2). Parameters with significant inter-observer reproducibility included junctional atypical lymphocytes (Fig. 1), architectural disarray (Fig. 2), spongiosis (Fig. 3), hyporefractile papillae (Fig. 4), and blood vessel dilatation, with  $p$ -values ranging from 0.867 to 0.156, respectively. Similarly, epidermal atypical lymphocytes, loss of demarcation and dendritic cells demonstrated homogeneity between investigators, with  $p$ -values from 0.156 to 0.069 in our analysis. Interestingly, for characteristic features such as vesicle-like structures (VES) (Fig. 5) and other features such as fibrosis, dermal atypical lymphocytes, and keratinocytes with elongated nuclei, no concordance between investigators was found (Table 2).

## 6 Distribution of RCM Parameters

$\text{Chi}^2$  analysis was performed following blinded image analysis by two independent investigators, blinded to diagnosis, name, age, and sex. The results demonstrated that selected features were present at particularly high frequency in individual skin diseases, with values ranging from 73 to 100% of all examined cases. It was shown that selected features are particularly

**Table 1** RCM Evaluation parameters and their morphologic description. Selected corresponding RCM features are shown in Figs. 1–4, respectively.

	RCM feature	Definition/description
Epidermal features		
1	Epidermal atypical lymphocytes	Small refractile round to oval cells 5 to 10 $\mu\text{m}$ in diameter scattered among spinous keratinocytes
2	Epidermal disarray	Loss of regular honeycomb pattern with loss of clear cell-to-cell demarcation and irregular cell size and morphology
3	Spongiosis	Increased intercellular brightness with accentuation of cell borders compared to normal skin
4	Loss of demarcation	Ill-defined cell borders, with associated thickening or blurring of intercellular spaces. May appear as focal, multifocal or diffuse.
5	Vesicle-like structures	Dark round-to-polycyclic intrapapillary structures, with more or less sharp demarcation to surrounding keratinocytes, containing scattered round to oval bright cells from 5 to 10 $\mu\text{m}$
6	Keratinocyte elongation of nuclei	Epidermal cells with dark, oval to oblong-shaped nuclei
7	Dendritic cells	Bright epidermal cells of stellate morphology/dendritic processes
Junctional features		
8	Junctional atypical lymphocytes	Small refractile round to oval cells 5 to 10 $\mu\text{m}$ in diameter lining up at the DEJ
9	Hyporefractile papillae	Dark appearance/loss of contrast from basal cells surrounding the dermal papillae
Dermal features		
10	Blood vessel dilatation	Bright canalicular structures with blood flow on <i>in vivo</i> examination, and notable dilatation in comparison with normal skin
11	Fibrosis	Increased number and disorganized distribution of bright, refractile fibrous bundles in upper papillary dermis
12	Dermal atypical lymphocytes	Small, refractile round to oval cells 5 to 10 $\mu\text{m}$ in diameter at the level of the papillary dermis.

**Table 2** Results of Cochran analysis are shown. Individual RCM parameters are shown with their respective *p*-values. Table presents ranking in decreasing order of *p*-value.

Rank	RCM feature	<i>p</i> value
1	Junctional atypical lymphocytes	0.867
2	Epidermal disarray	0.848
3	Spongiosis	0.811
4	Hyporefractile papillae	0.670
5	Blood vessel dilatation	0.420
6	Epidermal atypical lymphocytes	0.156
7	Loss of demarcation	0.093
8	Dendritic cells	0.069
9	Vesicle-like structures	0.030
10	Fibrosis	0.017
11	Dermal atypical lymphocytes	0.002
12	Keratinocyte elongation of nuclei	0.0001

frequent in MF, including spongiosis (94.7%), loss of demarcation (94.7%), and epidermal disarray (89.5%) (Table 3).

At the same time, however, other diagnoses such as Sezary Syndrome or lymphomatoid papulosis also show high prevalence of these features (Table 3), with frequencies reaching 100% for spongiosis, loss of demarcation, and epidermal disarray.

Both blinded investigators (INV I + II) showed comparable scores for features of spongiosis, loss of demarcation, disruption of the epidermal architecture, the presence of hyporefractile papillae, and epidermal atypical lymphocytes (Table 3). Lower, yet still comparable scores were found for keratinocytes with elongated nuclei, dendritic cells, and hole-like perforations. Interestingly, a marked difference between the two investigators was noted for the feature of vesicle-like structures (VES), whereby the respective values were 73.3% (INV I) and 52.6% (INV II).

## 7 Sensitivity/Specificity Analysis

Analysis was made following blinded image analysis by two investigators in correlation with the gold standard, routine histology, and in comparison with normal skin. Data from both investigators showed comparable rankings for selected parameters. Representative sensitivity/specificity data from INV I

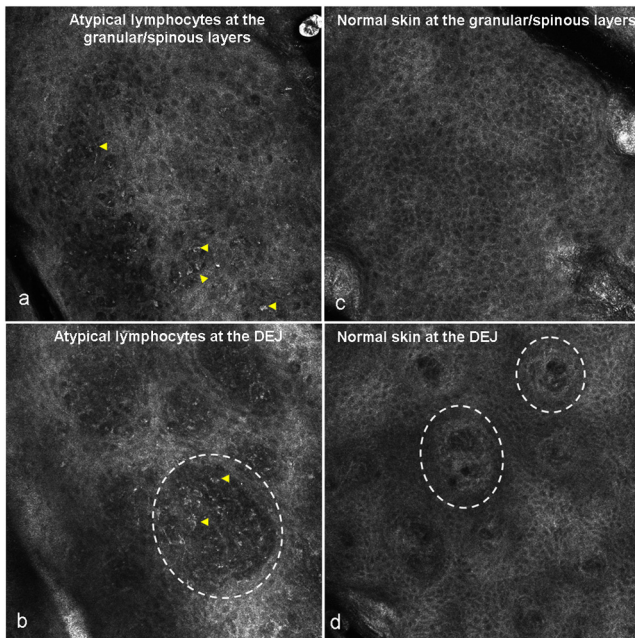


**Fig. 1** Panels (a) and (b) illustrate the presence of atypical lymphocytes in MF. Panel (a) demonstrates the presence of small to medium-sized bright round cells (yellow arrowheads) in between keratinocytes, which corresponds to exocytosis of lymphocytes on histopathologic examination. Panel (b) shows multiple bright round cells of varying morphology (yellow arrowheads) at the (DEJ) within the dermal papillae (white dashed circle). Panel (c) illustrates normal honeycomb pattern of the granular/spinous layer, and (d) shows the DEJ morphology with dermal papillae (white dashed circle) in absence of any inflammatory infiltrate. (Color online only.)

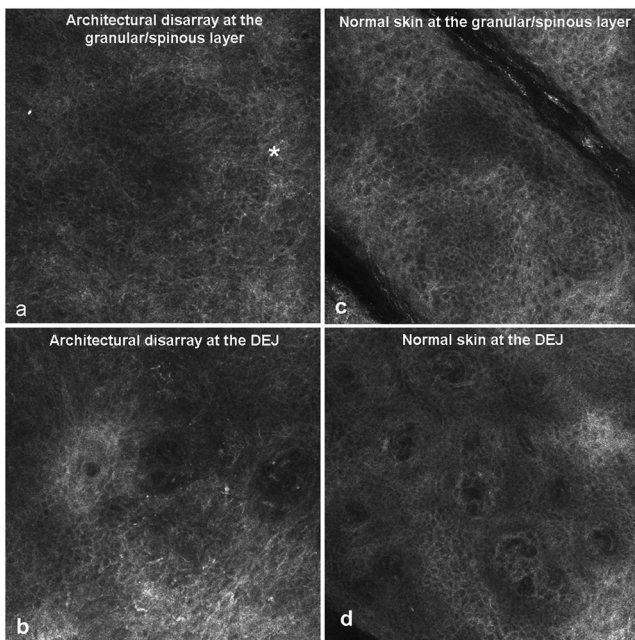


**Fig. 2** Panels (a) and (b) show architectural disarray appearing in lesions of MF. Panel (a) illustrates the disruption of the normal regular honeycomb pattern of the granular-spinous layer, displaying areas of dark reflectance in the center and blurred intercellular connection of the keratinocytes (white asterisk). Panel (b) shows RCM findings at the DEJ with the presence of inflammatory cells and aberrant morphology compared to normal skin as shown in panels (c) and (d).

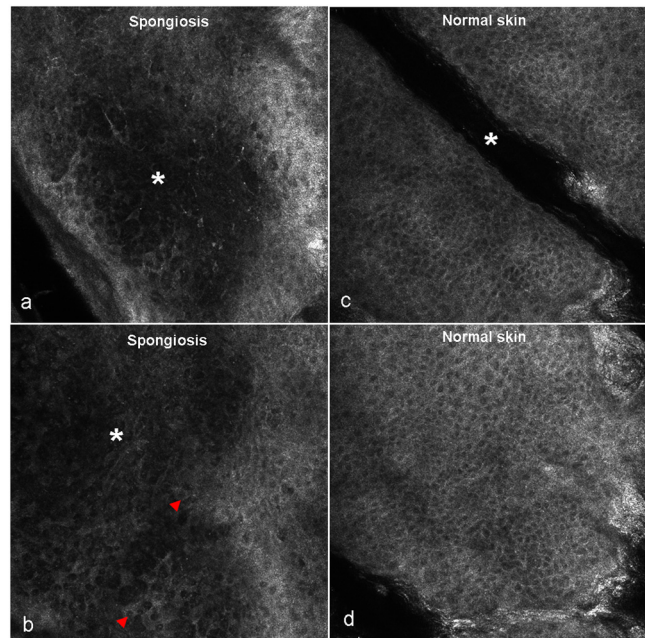


**Fig. 3** Panels (a) and (b) show representative images of MF illustrating RCM features of spongiosis. Panel (a) was obtained at the granular-spinous layer, demonstrating dark areas of low refractivity (asterisk), in which the delineation of the single cells and the overall honeycomb appearance of the epidermis is disrupted. Panel (b) shows a similar aspect (asterisk); furthermore, single keratinocytes with prominence of bright cytoplasm are noted (red arrowheads). Panel (c) shows normal granular layer of the epidermis with skin folds (asterisk) and, (d) illustrates typical honeycomb pattern of the spinous cell layer. (Color online only.)

are shown in Table 4. Features with high sensitivity/specificity included the presence of spongiosis (94.7% sensitivity/88.9% specificity for INV I; 100%/77.8% INV II, respectively), loss of demarcation (94.7%/88.9% INV I, 94.7%/77.8% INV II), and disruption of the epidermal architecture (89.5%/77.8% INV I, 100%/77.8% INV II). The feature of hyporefractile papillae and junctional/dermal atypical lymphocytes only demonstrated high specificity with limited sensitivity. Ultimately, a number of features demonstrated limited specificity and sensitivity, including dermal RCM features such as fibrosis and blood vessel dilatation.

While the ranking in order of the respective sensitivity/specificity values were comparable for both investigators for the majority of parameters, other parameters demonstrated marked differences, including vesicle-like structures (73.7/100 INV I vs 52.6%/88.9% INV II) and hole-like perforations (21.1/100% INV I vs 52.6%/88.9% INV II).

## 8 Discussion

The goal of this investigation was to re-evaluate the role of RCM in the analysis of cutaneous lymphoma. Based on diagnostic RCM criteria for MF that had previously been published,<sup>7</sup> we aimed to test their reproducibility, consistency, and distribution in a clinical study. Moreover, a sensitivity/specificity analysis was performed for those parameters that showed a high concordance in the initial evaluations.

While our findings are consistent with those previously reported, they also show that excellent or good inter-observer reproducibility may only be observed for selected parameters.

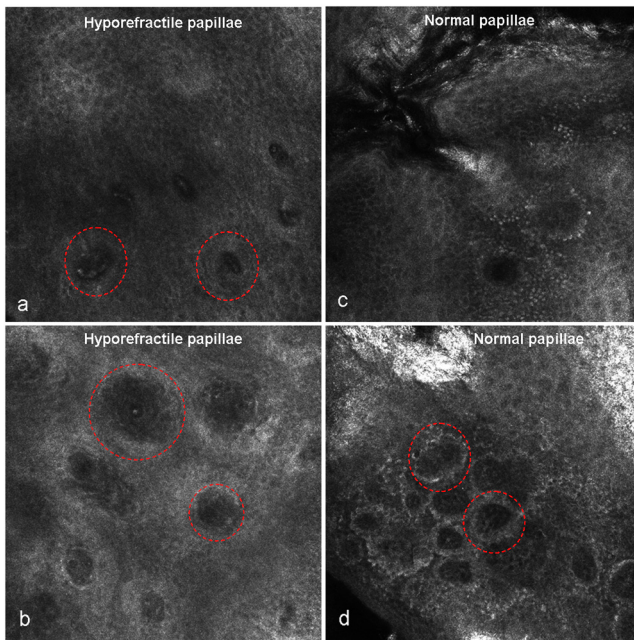


**Fig. 4** Panels (a) and (b) demonstrate RCM feature of hyporefractile papillae. Images were obtained at the DEJ and illustrate the absence of the bright rim of pigmented basal keratinocytes and melanocytes that is usually seen around the dermal papillae. Panels (c) and (d) illustrate normal, so-called edged papillae, which characteristically display a bright rim of small bright round cells around the dermal papillae. (Color online only.)

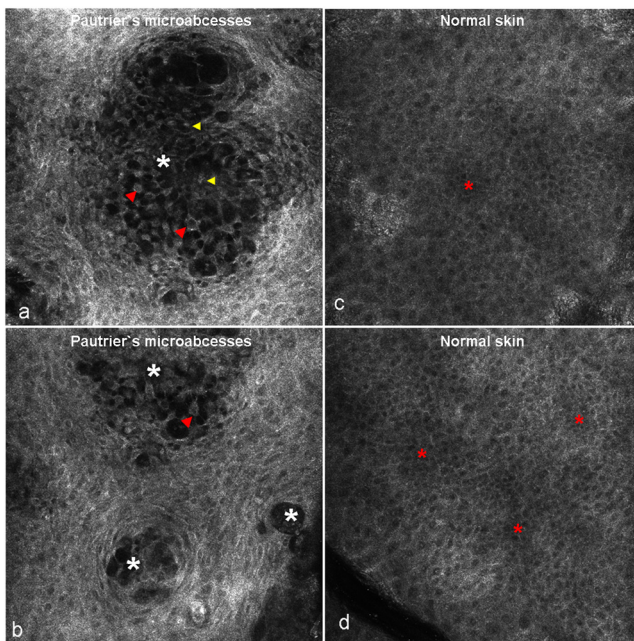


**Fig. 5** Panels (a) and (b) show representative images of Pautrier's MF in mycosis fungoides, illustrating multiple, well-circumscribed, vesicle-like areas of varying size and dark reflectance (asterisk) at the granular-spinous layers. Within these nonrefractile areas, remaining keratinocytes can be visualized (red arrowheads). These keratinocytes focally still show adherence by intercellular connections, but intercellular spaces are widely enlarged and the epidermal structure is disrupted. Furthermore, small bright cells representing inflammatory cells are noted (yellow arrowheads). Panels (c) and (d) demonstrate corresponding RCM findings of normal skin at the granular-spinous layers with typical honeycomb pattern. Areas that appear slightly darker than the surrounding epidermis represent areas with underlying dermal papillae. (Color online only.)

At the same time, the findings indicate that a broad clinical differential diagnosis must be considered when diagnostic RCM parameters are to be determined. This applies in particular to the RCM feature of spongiosis, which is the key feature of acute eczema and is present in a large variety of other inflammatory or proliferative skin disorders. In this study, spongiosis showed highest diagnostic sensitivity/specificity values, but regarding the large differential more parameters need to be considered. In that respect, a diagnosis of MF may only be made based on an integration of different RCM features, similar to routine histological evaluation. In that regard, it may be noted that other features such as loss of demarcation or the presence of epidermal disarray have not been described for acute contact dermatitis,<sup>11–14</sup> such that their presence may aid in the noninvasive diagnosis of MF based on RCM criteria. Since this study did not include cases of eczema, this important aspect will need to be the subject of a separate analysis.<sup>15,16</sup> A previous study by Ardigò et al. on the description of RCM findings of discoid lupus suggested the morphologic findings of epidermal disarray and ill-defined cell demarcation as being a variant of spongiosis.<sup>17</sup> While this feature lacks an unequivocal description, there is evidence that this aspect may be comparable to features observed in MF, namely “loss of demarcation,” “hole-like perforations,” and “epidermal disarray.”

The term atypical lymphocytes has been used in this publication, as has been suggested by previous authors correlating RCM features of MF with those established by routine histology.<sup>3–5</sup> Since RCM does not allow the visualization of nuclear atypia, the authors suggest a more descriptive terminology. Technical limitations of current RCM technology do not permit an accurate assessment of cell body-to-nuclei ratio, or specify other criteria of cellular atypia. Hence the term “bright roundish and large pleomorphic cells” may be used for description of what most likely corresponds to atypical lymphocytes in routine histology and that is consistent with the suggestion of a previous publication on the RCM evaluation of erythrodermic skin diseases including MF.<sup>18</sup>

Those features previously described as loss of demarcation/presence of epidermal disarray are more difficult to discern from mere spongiosis, since they do not actually have a histological correlate. Interestingly, in cases of contact dermatitis, the cell-to-cell demarcation is rather accentuated by the presence of intercellular edema, which increases refractility on RCM images. This obviously excludes areas of mere vesicle formation/vesiculation where local fluid accumulation leads to the distension of intercellular cohesion. The authors assume that these features may be different aspects on a continuous spectrum from mild spongiosis to progressive distension of keratinocytes with actual disruption of epidermal architecture.

Despite the heterogeneity of different studies, most authors agree on the fact that the presence of Pautrier's microabscesses is—if very characteristic—only present in approximately 19% to 37% of examined cases of MF, such that their absence does not necessarily indicate absence of disease.<sup>3–5</sup> In our study, we found that vesicle-like structures were present in 52% to 73% of all cases of MF (with no relevant inter-observer concordance, however). This may be attributed to the fact that differentiation between marked spongiosis and initial formation of Pautrier's microabscesses may be difficult to obtain by RCM evaluation. In this regard it can be explained that

**Table 3** Results of Chi<sup>2</sup> analysis are shown. The table shows the individual distribution of RCM parameters with respective diagnoses, following blinded image analysis by two independent investigators. Data expressed as presence of features in % of examined cases. A *p*-value of <0.05 was considered significant.

	MF	PARA	SEZ	LYP	NO
INVESTIGATOR 1					
Spongiosis	94.7 <sup>b</sup>	20	100	100	11.1
Loss of demarcation	94.7 <sup>b</sup>	0	100	100	11.1
Epidermal disarray	89.5 <sup>a</sup>	40	100	100	22.2
Hyporefractile papillae	78.9	20	100	100	11.1
Epidermal atypical lymphocytes	73.7 <sup>b</sup>	0	100	75	0
Vesicle-like structures	73.7	0	100	50	0
Junctional atypical lymphocytes	73.3 <sup>b</sup>	0	100	100	0
Keratinocyte elongation of nuclei	63.2	0	0	25	0
Dendritic cells	52.6	0	100	0	0
Hole-like perforations	21.2	0	50	25	0
INVESTIGATOR 2					
Spongiosis	100 <sup>b</sup>	0	100	75	22.2
Epidermal disarray	100 <sup>b</sup>	20	100	100	22.2
Loss of demarcation	94.7 <sup>b</sup>	20	100	100	22.2
Hyporefractile papillae	84.2 <sup>b</sup>	40	100	100	0
Junctional atypical lymphocytes	84.2 <sup>b</sup>	0	50	100	0
Epidermal atypical lymphocytes	68.4 <sup>a</sup>	0	100	75	0
Vesicle-like structures	52.6	0	100	25	11.1
Hole-like perforations	47.4	20	100	0	11.1
Keratinocyte elongation of nuclei	42.1	0	0	0	0
Dendritic cells	0	0	50	50	36.8

<sup>a</sup>*p* < 0,001.

<sup>b</sup>*p* < 0,0001.

one observer defined this finding as spongiosis, whereas the other interpreted it as Pautrier's microabscesses. For other features such as "hole-like perforations," "loss of demarcation," and "epidermal disarray," an exact distinction may be difficult to obtain due to the absence of specific descriptors.

There are several limitations to this study, the major one being the exclusion of cases of eczema, which may also be indistinguishable by histological analysis and thus poses a considerable challenge in the differential diagnosis. At the same time, this study is limited by the small sample size, narrowing the overall value of our results to those of a preliminary study. Technical limitations include limited resolution at deeper layers, which may contribute to the lack of reproducibility of respective dermal RCM features such as fibrosis, atypical dermal

lymphocytes, and blood vessel dilatation. These findings confirm those of a previous study by Pellacani et al., which also reported decreasing reproducibility for RCM features for melanocytic skin lesions at deeper anatomic skin levels.<sup>19</sup> Moreover, reduced reproducibility of selected features had been attributed to a possibly insufficient description of RCM features. With respect to this study, this may particularly apply to the features "hole-like perforations" and "keratinocyte elongation of nuclei."

Finally, costs for acquisition of the device and time for training need to be taken into consideration.

In summary, our findings are somewhat confirmatory of previous reports on the reproducibility of histopathological findings in MF and were also consistent with previously described RCM

**Table 4** Results of sensitivity/specificity analysis for RCM parameters are shown. Table presents ranking in order of 1) highest sensitivity 2) highest specificity, from scoring of investigator 1 (INV I). Only data with relevant reproducibility have been included in the analysis. Data are expressed as % of all examined cases. A  $p$ -value 0.05 was considered significant (Pearson  $\chi^2$  Test).

RCM parameter	SpecInv I	SensInv I	$p$ -value Inv I	Spec Inv II	Sens- Inv II	$p$ -value Inv II
Spongiosis	88.9%	94.7%	0.0001	77.8	100	0.0001
Loss of demarcation	88.9%	94.7%	0.0001	77.8	94.7	0.0001
Disarray of epidermis	77.8%	89.5%	0.0001	77.8	100	0.0001
Hyporefractile rings	88.9%	78.9%	0.001	100	84.2	0.0001
Junctional atypical lymphocytes	100%	73.7%	0.0001	100	84.2	0.0001
Vesicle-like structures (Pautrier's microabcesses)	100%	73.7%	0.0001	88.9	52.6	0.036
Epidermal atypical lymphocytes	100%	73.7%	0.0001	100	68.4	0.001
Blood vessel dilatation	77.8%	57.9%	0.077	100	78.9	0.0001
Dendritic cells	100%	52.6%	0.007	100	36.8	0.035

criteria by Agero et al. At the same time, the results show that RCM is a promising tool for evaluation of cutaneous lymphoma that allows the definition of discriminative features. Yet considering the broad differential diagnosis, any analysis must continue to be based on clinical and RCM morphological features, leading to diagnostic biopsy and molecular analysis in cases in which RCM morphology is suggestive of MF. Further studies including eczematous conditions are required and should aim at defining a diagnostic algorithm for the RCM diagnosis of MF and related conditions.

## References

1. R. Willemze et al., "WHO-EORTC classification for cutaneous lymphomas," *Blood* **105**, 3768 (2005).
2. D. Humme, A. Lukowsky, and W. Sterry, "Diagnostic tools in mycosis fungoides," *G. Ital. Dermatol. Venereol.* **145**(3), 375–384 (2005).
3. B. R. Smoller et al., "Reassessment of histologic parameters in the diagnosis of mycosis fungoides," *Am. J. Surg. Pathol.* **19**(12), 1423–1430 (1995).
4. C. Massone et al., "Histopathologic features of early (patch) lesions of mycosis fungoides: a morphologic study on 745 biopsy specimens from 427 patients," *Am. J. Surg. Pathol.* **29**(4), 550–560 (2005).
5. B. J. Nickoloff, "Light-microscopic assessment of 100 patients with patch/plaque-stage mycosis fungoides," *Am. J. Dermatopathol.* **10**(6), 469–477 (1988).
6. M. A. Weinstock and J. W. Horm, "Population-based estimate of survival and determinants of prognosis in patients with mycosis fungoides," *Cancer* **62**, 1658–1661 (1988).
7. A. L. Agero et al., "In vivo reflectance confocal microscopy of mycosis fungoides: A preliminary study," *J. Am. Acad. Dermatol.* **57**, 435–441 (2007).
8. M. Rajadhyaksha et al., "In vivo confocal scanning laser microscopy of human skin: melanin provides strong contrast," *J. Invest. Dermatol.* **104**, 946–952 (1995).
9. M. Rajadhyaksha, R. R. Anderson, and R. H. Webb, "Video-rate confocal scanning laser microscope for imaging human tissues in vivo," *Applied Optics* **38**, 1–12 (1999).
10. M. Rajadhyaksha et al., "In vivo confocal scanning laser microscopy of human skin II: advances in instrumentation and comparison with histology," *J. Invest. Dermatol.* **13**, 293–303 (1999).
11. S. Astner, S. González, and E. Gonzalez, "Noninvasive evaluation of allergic and irritant contact dermatitis by in vivo reflectance confocal microscopy," *Dermatitis* **17**(4), 182–191 (2006).
12. S. Astner et al., "Irritant contact dermatitis induced by a common household irritant: A noninvasive evaluation of ethnic variability in skin response," *J. Am. Acad. Dermatol.* **54**(3), 458–465 (2006).
13. S. Astner et al., "Pilot study on the sensitivity and specificity of in vivo reflectance confocal microscopy in the diagnosis of allergic contact dermatitis," *J. Am. Acad. Dermatol.* **53**(6), 986–992 (2005).
14. S. Astner et al., "Non-invasive evaluation of the kinetics of allergic and irritant contact dermatitis," *J. Invest. Dermatol.* **124**(2), 351–359 (2005).
15. A. B. Ackermann, T. S. Breza, and L. Capland, "Spongiotic simulants of mycosis fungoides," *Arch. Dermatol.* **109**, 218–220 (1974).
16. J. G. Orbaneja et al., "Lymphomatoid contact dermatitis: A syndrome produced by epicutaneous hypersensitivity with clinical features and a histopathologic picture similar to that of mycosis fungoides," *Contact Dermatitis* **2**, 139–143 (1976).
17. M. Ardigo et al., "Preliminary evaluation of in vivo reflectance confocal microscopy features of discoid lupus erythematosus," *Br. J. Dermatol.* **156**(6), 1196–1203 (2007).
18. S. Koller et al., "In vivo reflectance confocal microscopy of erythematous skin diseases," *Exp. Dermatol.* **18**(6), 536–540 (2009).
19. G. Pellacani et al., "Reflectance confocal microscopy and features of melanocytic lesions: an internet-based study of the reproducibility of terminology," *Arch. Dermatol.* **145**(10), 1137–1438 (2009).